PHYSICAL REVIEW B **67**, 115306 (2003)

Adsorption of N-containing species onto SiC(0001) surfaces: A theoretical study

J. Olander and K. M. E. Larsson
Department of Materials Chemistry, The Ångstrom Laboratory, Uppsala University, Box 538, 751 21 Uppsala, Sweden

(Received 6 September 2002; published 6 March 2003)

Adsorption of nitrogen-containing species onto the Si and C surfaces of SiC(0001) has been theoretically investigated, using density functional theory calculations under periodic boundary conditions. The idea was then to investigate nitrogen incorporation during *in situ* doping of SiC. As a guide to the composition of gaseous species above a growing SiC surface, earlier results from thermodynamic calculations, performed at experimental conditions for N *in situ* doping, were used. The present results show that adsorption of N_2, N, NH_3, NH_2, CN, HCN, HNC, H_2CNH, SiN, SiNH, and Si_2N, with three exceptions, is exothermic to both SiC surfaces. The exceptions include adsorption of NH_3 or the N atom in HCN or HNC to the C surface. The twofold adsorption processes were all found to be exothermic and more favorable for the Si than for the C surface. Furthermore, adsorption by the N(Si) atom in the adsorbate was found to be stronger to the Si(C) surface while the adsorbates seem to bind equally strongly to both surfaces by the C atom. There was generally a clear correlation between larger adsorption energies, shorter bond lengths and higher bond overlap populations in the region between the bonding atoms.

DOI: 10.1103/PhysRevB.67.115306 PACS number(s): 68.43.Bc, 61.72.Ww

I. INTRODUCTION

Silicon carbide has a large potential for high-temperature, high-power, and high-frequency devices. However, there are several technological difficulties that must be overcome before realizing SiC devices for electronic applications. The development of appropriate doping processes is very important in fabricating low-resistivity crystals. It would then be valuable to obtain a better knowledge about the doping mechanisms in order to be able to control the dopant incorporation better. Nitrogen is the most common *n*-type dopant of SiC. Unlike silicon, silicon carbide cannot be efficiently doped by a diffusion process.[1] Reproducible doping of SiC is accomplished *in situ* during epitaxial growth of the material.

The conventional growth direction of SiC is [0001], for which the Si and C planes have different polarities [the electronegativity (e.n.) of Si is 1.9, e.n.(C)=2.6 and e.n.(N)=3.0].[2] This leads to different conditions for nitrogen incorporation into the two surfaces. The different polytypes will, due to similar stacking sequences of the topmost atomic layers in the [0001] direction, only slightly influence the surface geometry.[3] For this reason, the SiC(0001) surface that has been investigated in the present study can be considered to be either 3C-SiC(111), 4H-SiC(0001), or 6H-SiC(0001). Hydrogen atoms have been found to effectively saturate the surface dangling bonds of SiC(0001),[4] and thereby maintain the (1×1) structure of the surface atoms. Furthermore, the sticking coefficient of N has been found to be higher at steps than on flat SiC(0001) surfaces. It has even been claimed to be unity at steps.[5] The doping process is usually performed on a surface with an off-angle from the (0001) plane. However, a typical off-angle of 3.5° (for 6H-SiC) or 8° (for 4H-SiC), is identical to a surface step every 15th or 7th unit cell. Hence, although the off angle might be highly important for the overall incorporation process, the initial adsorption of a gaseous species is most likely to occur on a terrace between two surface steps.

The size of the nitrogen atom will allow it to occupy either the C- or the Si-site of SiC without sterical hindrances [$r_{\text{cov}}(\text{N})=0.73$ Å, $r_{\text{cov}}(\text{C})=0.77$ Å, and $r_{\text{cov}}(\text{Si})=1.16$ Å],[2] but the C-site of the SiC lattice has generally been found to be the preferred site of nitrogen atoms.[6,7] Reproducible *n*-type dopant incorporation (from below 10^{14} to 10^{19} cm^{-1}) into SiC has been obtained by using the site-competition epitaxial technique introduced by Larkin.[8] This technique is based on intentional variations of the C/Si ratio of the precursors during epitaxial growth. For the Si-face of SiC, N incorporation has been found to decrease with an increased C/Si ratio (despite constant N_2 flow), while N incorporation into the C face has been found to be independent of the C/Si ratio.[5,9] For the Si surface, the N-containing species are then generally believed to be ''out-competed'' by the high concentration of the carbon growth species.

Nitrogen doping of SiC(0001) has experimentally been investigated in a recently published paper by Forsberg and co-workers.[9] In their article they use thermodynamic calculations to estimate the the equilibrium composition of gaseous species above the growing SiC surface at their typical growths conditions. With guidance from these thermodynamic considerations, adsorption processes of various N-containing gaseous species are presently investigated, using first principles calculations.

II. METHODS

The adsorption energies were calculated using the following equation:

$$\Delta E_{\text{ads}}(A)=E(A)+E(\text{surf})-E(\text{surf}-A), \tag{1}$$

where $E(\text{surf-}A)$ and $E(\text{surf})$ are the calculated total energies of the surface with or without an adsorbate, respectively. $E(A)$ is the total energy of the adsorbate. These calculations were based on the density functional theory (DFT).[10,11] DFT methods use various approximations to describe the exchange and correlation interactions between the electrons.

The commonly used local density approximation (LDA) rather accurately describes local properties such as bond lengths and vibration frequencies. The more accurate generalized gradient approximation (GGA) methods involve an extended treatment of inhomogeneities in the electron density, resulting in improved results of the global changes in energy (e.g., bond energies). Quantum mechanical calculations are performed at zero K. However, an adsorption energy may differ at higher temperatures. If the difference between two adsorption energies is larger than 1 eV at 0 K, their relative order is here supposed to be retained at experimental temperatures. The CASTEP (Cambridge Sequential Total Energy Package) computer program package from Accelrys, has been used in the present study.

The GGA/GGS functional developed by Perdew-Wang (PW91)[12] was used for the geometry optimizations in order to obtain reliable bond energies as well as reliable geometries. The atoms were then represented by nonlocal ultrasoft pseudopotentials in the Kleinman-Bylander separable form.[13] Furthermore, the electronic wave functions were expanded in terms of plane waves. The Monkhorst-Pack scheme generated 1 *k* point in representing the electronic wave function of the system.[14] The cutoff energy used for the plane-wave basis set was 200 eV. As a verification of this basis set and *k*-point sampling, the adsorption energy of NH_2 was also calculated using 2 *k* points and a cutoff energy of 240 eV. Since the difference in adsorption energies obtained, using these various levels of accuracy [472(2 *k* points) vs 508(1*k* point)], was numerically too small to alter a well-defined order of adsorption energies, 1 *k* point and a cutoff energy of 200 eV was found adequate to use in the present study.

In order to investigate the bonding characteristics of the different species, an electron population analysis was carried out. The overlap population gives the amount of charge within the bonding region between two atoms and is a measure of the strength of a covalent bonding. Overlap populations related to the chemisorbed species and bonding surface atoms were calculated by the formalism described by Segall and co-workers.[15] The wave functions were then initially projected from plane waves to a localized orbital basis set. One measure of the quality of the projection is the value of the spilling parameter which for the present calculations was in the order of 0.01, thus indicating a good representation of the basis set. As a test of the reliability of the LCAO basis set used, the Si *d* orbitals were included (using 5 *k* points) in addition to the *s* and *p* orbitals when calculating the overlap population for SiN^{Si}. (The superscript Si signifies adsorption to the Si surface.) However, this increase in localized basis set resulted in numerical changes of less than 8% in overlap population. This difference is acceptable, considering that we are dealing with relative, in contrast to absolute, magnitudes of the overlap populations. The shortening $r_1^{\mathrm{Si}}(A)$ is the distance between the adsorbate (A) and the bonding surface atom, $\mathrm{pop}[r_1^{\mathrm{Si}}(A)]$ denote the overlap population in the bonding region.

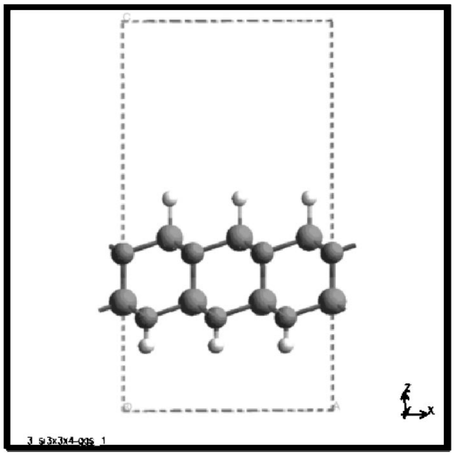

FIG. 1. A side view of the ideal bulk structure model of SiC(0001) initially used during the calculations. The larger, medium (gray) and small circles represent Si, C, and H atoms, respectively. By interchanging the Si and C atoms one obtains the 4H-SiC(000) model cell.

Periodically repeated unit cells, consisting of four atomic layers, were used in modeling the SiC surfaces (Figs. 1,2). Each layer contained 9 Si (or C) atoms and the distance between the two-dimensional slabs was 9 Å. The bottom and uppermost layers of these slabs were hydrogen terminated. Geometries for ideal on-top adsorption were in each case taken as a starting point for the calculations. The closest atomic neighbor (in all directions) of the adsorbate-bonding surface Si (C) atom was allowed to relax during the geometry optimizations. The rest of the unit cell was kept fixed in order to hold the characteristics of a more realistic surface. To examine the optimal size of the unit cell used in the present investigation, the adsorption energy of SiN was calculated using a slab consisting of six (instead of four) atomic layers. In these calculations, all neighboring atoms two bonding-distances away from the adsorbate-bonding surface atom, were allowed to relax. As an additional test, the two-fold adsorption of HCN to a four-layer slab, extended in the x-direction to contain 12 surface atoms (instead of 9), was calculated. The calculated adsorption energies of SiN and

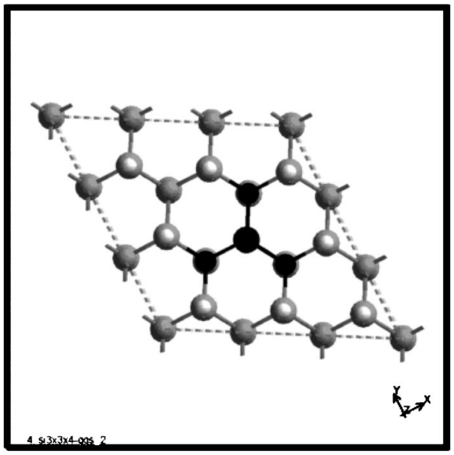

FIG. 2. A top view of the bulk structure model of SiC(0001). The black atoms note those that were allowed to relax during the geometry optimization calculations. $\nu_{\text{C-Si-C}}$ marks the angle that was measured in order to how well sp^3 hybridized the surface atom was after geometry optimization.

HCN differed by less than 1 and 4%, respectively. The smaller size of unit cell was, hence, considered to be adequate to use in the present study.

III. RESULTS AND DISCUSSION

A. General

1. Thermodynamics

In a recently published paper, Aigo and co-workers[16] assumed the nitrogen dopant molecule to decompose into monoatomic nitrogen radicals on the SiC surface and thereafter incorporate into the SiC surface. However, during a CVD process, the nitrogen molecules may very well react with the gas phase SiC precursors prior to any adsorption to the growing surface. In order to obtain more information about the gas phase composition during the nitrogen doping process, thermodynamic calculations have been considered. The gaseous composition in the reactor has been calculated by Forsberg and co-workers for their experimental conditions of thermally activated CVD during in situ nitrogen doping of SiC.[9] Charged radical precursors that can be present in more energetic deposition processes (e.g., CVD involving ion bombardment) were not taken into account. The following order of abundance of the N-containing species in the gas phase above the growing surface was then obtained:

$$N_2(10^{-4}) > HCN(10^{-5}) \sim SiNH(10^{-5}) > HNC(10^{-6}) > Si_2N(10^{-7}) > NH_3(10^{-8}) \gg SiN(10^{-10}) \gg N(\sim 10^{-12}). \tag{2}$$

The numbers within parenthesis are the approximate partial pressures (in atm) of the different gas phase species. According to these calculations, the concentration of nitrogen radicals (N) is expected to be low in the CVD reactor. In order to model the reactor atmosphere close to the growing surface, additional thermodynamic calculations were performed in which solid SiC was allowed to form. The following order was then obtained:

$$N_2(10^{-4}) > HCN(10^{-5}) > HNC(10^{-6}) > NH_3(10^{-7}) > NH_2(10^{-9}) > H_2CNH(10^{-10}) \sim CN(10^{-10}) \sim SiNH(10^{-10}) \gg N(10^{-12}). \tag{3}$$

There are various explanations for the differences between Eqs. (2) and (3). As can be seen in Eq. (3), the concentrations of SiNH, Si_2N, and SiN decrease close to the surface while the concentrations NH_3, NH_2, H_2CNH, and CN were found to increase. A result from both calculations is that the concentration of nitrogen radicals is estimated to be very low (i.e., about 10^8 times lower than that of N_2).

2. Surface reactions

Thermodynamic calculations give an indication of which gaseous species that can be expected in the gaseous atmosphere during CVD, and in which relative concentrations. These calculations give general information, but they are performed for equilibrium states and do not include the kinetics of a system. Moreover, they do not comprise surface reactions. If N_2, which is expected to be the most abundant N-containing species in the gas phase (according to Sec. III A 1), adsorbs very strongly, it will probably be the dominant species for nitrogen incorporation. Other nitrogen-containing species may, however, adsorb more favorably than N_2, and influence the dopant process to various extents. For this reason, the adsorption processes of the gaseous species presented in Eqs. (2), (3) have been investigated in the present study. Onefold adsorption of each of the non-H atoms in the gaseous species, as well as twofold adsorption, was individually studied for the adsorbates. For the sake of clarity, the various adsorbates are here presented in three different groups: (i) N_2, N, NH_3, NH_2, (ii) CN, HCN, HNC, H_2CNH, and (iii) SiN, SiNH, and Si_2N.

TABLE I. Calculated energies (kJ/mol) for adsorption to the Si or C surface of SiC(0001). In the cases where two different elements in the adsorbate can bond onefoldly to the surface, the one that was considered as the adsorbing element is written in boldface.

	Si-surface		C-surface	
	onefold	twofold	onefold	twofold
N_2	160	247	80	144
N	426		474	
NH_3	127		−9	
NH_2	508		369	
C**N**	496	463	394	522
CN	503	463	511	522
HC**N**	103	300	0	220
H**C**N	70	300	68	220
H**N**C	44	225	−41	169
HN**C**	120	225	110	169
H_2C**N**H	164	395	43	236
H_2**C**NH	62	395	46	236
Si**N**	650	662	546	561
SiN	340	662	385	561
Si**N**H	235	453	122	391
SiNH	144	453	211	391
Si_2**N**	348	494	250	393
Si_2N	283	494	402	393

B. Adsorption of N_2, N, NH_3, NH_2

1. Onefold adsorption

The first group of adsorbates considered is composed of species containing only nitrogen and hydrogen atoms. The calculated energies for adsorption to SiC(0001) surfaces are presented in Table I. The numerical order of energies obtained for onefold adsorption of N_2, N, NH_3, and NH_2 to the Si surface is

$$NH_2(508) > N(426) > N_2(160) > NH_3(127). \tag{4}$$

TABLE II. The distance between the adsorbate and the surface r_1 (Å), the overlap population in the bonding region pop$[r_1]$ ($|e|$) and the angle between the adsorbate-bonding surface Si(C) atom and its closest C(Si) neighbors $\nu_{\text{C-Si-C}}$ ($\nu_{\text{Si-C-Si}}$) (deg).

	Si surface			C surface		
	r_1	pop$[r_1]$	$\nu_{\text{C-Si-C}}$	r_1	pop$[r_1]$	$\nu_{\text{C-Si-C}}$
Term.	1.51	0.94	110.7	1.12	0.80	111.3
Rad.			112.6			115.6
Dirad.			113.5			114.9
			/113.3			/115.0
N$_2$(**N**N)	1.77	0.54	112.5	1.52	0.52	110.2
N$_2$(**NN**)	1.93	0.47	110.7	1.61	0.47	109.9
	/1.95	/0.46	/111.2	/1.65	/0.43	/110.1
N	1.75	0.65	111.4	1.34	0.82	109.0
NH$_3$	2.02	0.14	115.5	1.62	0.23	111.4
NH$_2$	1.68	0.71	110.3	1.48	0.57	110.4

The values within parenthesis represent the adsorption energies in kJ/mol. The corresponding order for the C surface is

$$\text{N}(474) > \text{NH}_2(369) > \text{N}_2(80) > \text{NH}_3(-9). \qquad (5)$$

Accordingly, chemisorption of N and NH$_2$ was found to be strongly exothermic to both the Si and C surfaces. The N radical was found to bind somewhat stronger to the C surface, while adsorption of NH$_2$ was stronger to the Si surface. Moreover, the adsorption energies of N$_2$ and NH$_3$ were much smaller, with somewhat larger values for the Si surface. The adsorption of NH$_3$ to the C surface was even found to be endothermic. One explanation to the lower adsorption energies for N$_2$ and NH$_3$ is that these species are energetically very stable in their gaseous forms. As a consequence, they do not gain much energy while altering their electronic configurations when binding to a surface. Furthermore, in order to maintain the correct structure of the growing SiC material, it is important to hold the sp^3 hybridization of the surface atoms. Upon adsorption of N, NH$_2$, and N$_2$, the surface atoms (the adsorption sites) were, with two exceptions, fairly well sp^3 hybridized, since $\nu_{\text{C-Si-C}}/\nu_{\text{Si-C-Si}} = 109.0$–$110.4°$ (Table II). The exceptions include an influence of sp^2 hybridization on the surface atom after adsorption of N and N_2 to the Si surface ($\nu_{\text{C-Si-C}} = 111.4$–$112.5°$). There is also a strong influence of sp^2 hybridization after adsorption of NH$_3$ to the Si(C) surface, with $\nu_{\text{C-Si-C}}$ $(\nu_{\text{Si-C-Si}}) = 115.5(111.4)°$. Accordingly, the adsorption reactions of N and N$_2$ to the Si surface were, from a geometrical point of view, not found to be optimal in spite of the large adsorption energy of N.

The lower adsorption energies generally correspond to longer bond lengths and smaller overlap populations in the bonding region. For example, the values obtained for adsorption of NH$_3$ ($\Delta E_{\text{ads}} = 127$ kJ/mol, $r_1 = 2.02$ Å, pop$[r_1] = 0.14$ $|e|$) and NH$_2$ ($\Delta E_{\text{ads}} = 508$ kJ/mol, $r_1 = 1.68$ Å, pop$[r_1] = 0.71$ $|e|$) to the Si surface illustrate this circumstance very well. However, according to r_1 and pop$[r_1]$, the N$_2$ bond to the Si(C) surface was found to be only slightly weaker than the N(NH$_2$) bond in spite of a much smaller adsorption energy (Tables I,II). Furthermore, the N$_2$ adsorbate is, compared to the other species within this group of adsorbates, more exceptional since it contains an internal triplet bond. A variation in length of this bond will result in a change in internal bond strength and, hence, a corresponding change in energy of adsorption. The internal distance (r_2) between the nitrogen atoms was in the present study calculated to be longer for the adsorbed (ads) N$_2$ molecule compared to the gaseous (gas) molecule $[r_2(\text{ads}) - r_2(\text{gas}) = 0.05\ (0.08)$ Å$]$, with a corresponding lowering of the overlap population $[\text{pop}[r_2(\text{ads})] - \text{pop}[r_2(\text{gas})] = -0.29$ (-0.30) $|e|]$, see Table III. Hence, the strong triple bond of gaseous N$_2$ was appreciably weakened as a result of adsorption to the two different types of surfaces. This fact strengthens the indication from the (r_1) overlap populations that the bonds formed between N$_2$ and each of the two surfaces are stronger than the corresponding adsorption energies imply.

TABLE III. The distance between the atoms in the adsorbate r_2 (Å) and the corresponding overlap population pop$[r_2]$ ($|e|$).

	Si surface		C surface	
	r_2	pop$[r_2]$	r_2	pop$[r_2]$
N$_2$	1.13	1.38	1.13	1.38
N$_2$(**N**N)	1.20	1.09	1.21	1.08
N$_2$(**NN**)	1.25	1.03	1.26	1.06
NH$_3$	1.01	0.63	1.01	0.63
NH$_3$	1.02	0.67	1.05	0.23
NH$_2$	1.02	0.57	102	0.57
NH$_2$	1.01	0.70	1.01	0.72

2. Twofold adsorption

In order to obtain twofold adsorption of a gas phase species to any of the SiC(0001) surfaces, two neighboring vacancies have to be created on the surface. This can be accomplished in two different ways. The gaseous species can directly create two bonds to a diradical surface site. Such diradical sites are assumed to occur on the isostructural diamond (111) surface,[17] but they are expected to be less abundant compared to single radical sites. An alternative mechanism of twofold adsorption involves the formation of a vacant surface site adjacent to the onefoldly chemisorbed species. The adsorbate then bends over to the radical surface site and becomes twofoldly adsorbed. This mechanism is, of course, totally dependent on the thermodynamics of the preceding onefold adsorption as well as on the energy barrier when going from onefold to twofold adsorption.

The adsorption energy of the twofoldly adsorbed N$_2$ was more favorable for the Si (247 kJ/mol) compared to the C surface (144 kJ/mol). However, neither of these adsorption reactions is strongly exothermic, considering the fact that two bonds are formed by twofold adsorption. After adsorption, the binding surface C atoms were almost sp^3 hybridized, while there was an influence of sp^2 hybridization on the corresponding Si atoms. The bonds to the Si(C) surface of twofoldly adsorbed N_2 were found to be longer than the corresponding onefold bonds $[r_1(\mathrm{N_2,two\text{-}fold}) - r_1(\mathrm{N_2,onefold}) = 0.17\ (0.11)\ \text{Å}]$, and to have smaller accompanying overlap populations $[\mathrm{pop}[r_1(\mathrm{N_2,two\text{-}fold})] - \mathrm{pop}[r_1(\mathrm{N_2,one\text{-}fold})] = -0.05 - 0.11\ |e|]$, see Table II. Hence, the bonds between the surface and the adsorbate are weaker in the former case. This result agrees with the fact that the adsorption energy per bond was found to be larger for onefold $[\Delta E_{\mathrm{ads}}(\mathrm{N_2})/\mathrm{bond} = 160\ (80)\ \mathrm{kJ/mol}]$ compared to twofold adsorption $[\Delta E_{\mathrm{ads}}(\mathrm{N_2})/\mathrm{bond} = 124\ (72)\ \mathrm{kJ/mol}]$ to the Si(C) surfaces (Table I).

3. Discussion

The present results predict strong chemisorption of N and NH_2 to the investigated SiC(0001) surfaces. Moreover, the bonding surface atoms were found to be well sp^3 hybridized for these adsorbates, except for a slight sp^2 hybridizion of the surface Si atom upon N adsorption. Adsorption of NH_3 was found to be weakly exothermic (endothermic) for the Si (C) surface. Furthermore, the onefold-twofold adsorption of N_2 was slightly more promising with larger bond strengths for the Si surface compared to the C surface. For each surface, the bond of onefoldly adsorbed N_2 was stronger than the individual bonds of twofoldly adsorbed N_2. Generally, the N_2 molecule was stretched (by 0.07–0.13 Å) as a result of adsorption to the surfaces, which is promising for atomic N incorporation into the SiC material.

During N *in situ* doping, N_2 is expected to be the most abundant of the N-containing gaseous species in the gaseous atmosphere above the growing SiC surface at equilibrium [Eqs. (2), (3)]. Moreover, the concentration of NH_3 is expected to be $10^3 - 10^4$ times lower than that of N_2. Generally, bonds are expected to become weaker with an increase in temperature. It is, hence, in the present study difficult to predict the probability for adsorption at experimental temperatures. Furthermore, the gas phase concentrations of N and NH_2 at equilibrium are estimated to be 10^5 and 10^8 times lower, respectively, than the concentration of N_2 during SiC growth [Eqs. (2),(3)]. For this reason, the N and NH_2 species are not expected to be of any major importance for nitrogen incorporation into SiC at thermodynamic equilibrium conditions. However, it is important to keep in mind that although thermodynamic calculations give good indications, the gases in a CVD reactor are not in equilibrium. In addition, activation of the precursor gas during deposition (e.g., by laser or hot filament) can change the composition of gaseous species significantly. Hence, gaseous species that are much less abundant at equilibrium (such as N and NH_2) cannot be completely ruled out to be important contributors for nitrogen doping.

C. Adsorption of HCN, HNC, CN, H_2CNH

1. Onefold adsorption

Adsorption processes of CN, HCN, HNC, and H_2CNH to the SiC(0001) surfaces have also been investigated in the present study and the adsorption energies are presented in Table I. For the situations with two conceivable atoms in the adsorbate, the atom written with a bold-faced letter is being bonded to the surface atom. The numerical order of the obtained energies for onefold adsorption onto the Si surface is

$$\begin{aligned}&\mathbf{C}\mathrm{N}(503) \sim \mathrm{C}\mathbf{N}(496) > \mathrm{H_2C}\mathbf{N}\mathrm{H}(164) > \mathrm{HN}\mathbf{C}(120)\\&> \mathrm{HC}\mathbf{N}(103) \sim \mathrm{H}\mathbf{C}\mathrm{N}(70) \sim \mathrm{H_2}\mathbf{C}\mathrm{NH}(62)\\&\sim \mathrm{H}\mathbf{N}\mathrm{C}(44).\end{aligned} \tag{6}$$

The corresponding order for the C surface is

$$\begin{aligned}&\mathbf{C}\mathrm{N}(511) > \mathrm{C}\mathbf{N}(394) > \mathrm{HN}\mathbf{C}(110) > \mathrm{H}\mathbf{C}\mathrm{N}(68)\\&\sim \mathrm{H_2}\mathbf{C}\mathrm{NH}(46) \sim \mathrm{H_2C}\mathbf{N}\mathrm{H}(43)\mathrm{HC}\mathbf{N}(0)\\&> \mathrm{H}\mathbf{N}\mathrm{C}(-41).\end{aligned} \tag{7}$$

The chemisorption processes of CN to the SiC surfaces were found to be energetically very favorable. Adsorption of **H**N**C** to either surface, as well as adsorption of $\mathrm{H_2C\mathbf{N}H}$ or HC**N** to the Si surface, was also found to be exothermic. For the remaining species ($\mathrm{HC\mathbf{N}^{C}}$, $\mathrm{H\mathbf{C}N^{Si,C}}$, $\mathrm{H\mathbf{N}C^{Si,C}}$, $\mathrm{H_2C\mathbf{N}H^{C}}$, $\mathrm{H_2\mathbf{C}NH^{Si,C}}$), the adsorption reactions were calculated to be only slightly exothermic or endothermic. Generally, in the situations where the C atom in the adsorbate was bonded to the surface, the adsorption energy obtained for each adsorbate (**C**N, H**C**N, HN**C** and $\mathrm{H_2\mathbf{C}NH}$) was similar for the Si and C surfaces (with differences of less than 16 kJ/mol). However, adsorption of the N atom in the adsorbate was in each case (C**N**, H**N**C, HC**N**, and $\mathrm{H_2C\mathbf{N}H}$) more favorable for the Si surface compared to the C surface (with differences of 85–121 kJ/mol). After adsorption of C**N**, **C**N, $\mathrm{H\mathbf{C}N^{Si}}$, $\mathrm{HN\mathbf{C}^{Si}}$, or H**N**C, the sp^3 hybridization of the binding surface atom was influenced by sp^2 hybridization, according to the angles $\nu_{\text{C-Si-C}}/\nu_{\text{Si-C-Si}} = 111.0–112.5°$ (Table IV). On the contrary, the binding surface atom was sp^3 hybridized after adsorption of HC**N**, $\mathrm{H\mathbf{C}N^{C}}$, $\mathrm{HN\mathbf{C}^{C}}$, $\mathrm{H_2C\mathbf{N}H}$, or $\mathrm{H_2\mathbf{C}NH}$ to the Si(C) surface $(\nu_{\text{C-Si-C}}/\nu_{\text{Si-C-Si}} = 108.3–110.8°)$. This means that the energetically most favorable adsorption reactions (i.e., those of CN) do not result in optimal surface geometries.

Generally, the strong adsorption energies presently obtained correspond to short bonds with large overlap populations. An exception is the bonding distance of **C**N(C**N**) to the Si surface, which was found to be longer [by 0.06(0.01) Å], with a smaller [by $-0.12(-0.11)\ |e|$] corresponding overlap population, than that obtained for HN**C**(HC**N**) in spite of a larger adsorption energy [by 383(426) kJ/mol] in the former case. Moreover, the bonds of C**N**(**C**N) and HC**N**(HN**C**) to the C surface were similar (with differences smaller than 0.00(0.07) Å and 0.01(0.05)$|e|$, Table IV], although the adsorption energy of C**N**(**C**N) was larger [by 394(401) kJ/mol] than that of HC**N**(HN**C**). Hence, the bonds of HN**C** and HC**N** to both surfaces seem to be stronger (or similar in strength) compared to the corresponding bonds formed by **C**N and C**N**, in spite of much larger adsorption energies of the two latter adsorbates. As was discussed in Sec. III B 1, the adsorption energy does not only comprise

TABLE IV. The distance between the adsorbate and the surface r_1 (Å), the overlap population in the bonding region pop[r_1](|e|) and the angle between the adsorbate-bonding surface Si(C) atom and its closest C(Si) neighbors $\nu_{\text{C-Si-C}}$ ($\nu_{\text{Si-C-Si}}$) (deg). Where two atoms in the adsorbate bind to the surface, the values corresponding to the N atom in the adsorbate are listed first.

	Si surface			C surface		
	r_1	pop[r_1]	$\nu_{\text{C-Si-C}}$	r_1	pop[r_1]	$\nu_{\text{Si-C-Si}}$
Term.	1.51	0.94	110.7	1.12	0.80	111.3
Rad.			112.6			115.6
Dirad.			113.5			114.9
			/113.3			/115.0
C**N**	1.72	0.54	112.5	1.41	0.68	111.2
CN	1.86	0.72	111.7	1.41	0.94	111.4
CN	1.84	0.52	110.7	1.41	0.93	111.5
	/1.86	/0.70	/110.7	/	0.93	/115.7
HC**N**	1.71	0.65	110.8	1.41	0.69	110.2
H**C**N	1.92	0.64	111.3	1.56	0.71	110.6
H**CN**	1.78	0.64	109.2	1.55	0.57	109.7
	/1.99	/0.71	/109.8	/1.58	/0.74	/107.8
H**N**C	1.80	0.48	112.1	1.64	0.43	111.0
HN**C**	1.80	0.84	111.2	1.44	0.89	109.1
H**NC**	1.89	0.50	110.1	1.71	0.36	108.9
	/1.93	/0.75	/111.2	/1.53	/0.81	/110.6
H_2C**N**H	1.72	0.69	110.8	1.48	0.64	109.2
H_2**C**NH	1.96	0.59	110.8	1.57	0.72	108.3
H_2**CN**H	1.73	0.76	109.6	1.53	0.59	108.5
	/1.92	/0.74	/109.0	/1.60	/0.71	/109.6

TABLE V. The distance between the non-H atoms in the adsorbate r_2 (Å) and the corresponding overlap population pop[r_2] (|e|).

	Si surface		C surface	
	r_2	pop[r_2]	r_2	pop[r_2]
CN	1.17	1.61	1.17	1.61
C**N**	1.17	1.44	1.18	1.47
CN	1.16	1.74	1.16	1.80
CN	1.23	1.38	1.16	1.79
HCN	1.15	1.73	1.15	1.73
HC**N**	1.22	1.24	1.23	1.23
H**C**N	1.23	1.29	1.24	1.29
H**CN**	1.28	1.24	1.30	1.27
HNC	1.17	1.38	1.17	1.38
H**N**C	1.26	0.93	1.25	1.04
HN**C**	1.21	1.31	1.23	1.34
H**NC**	1.31	1.05	1.31	1.13
H_2CNH	1.26	1.12	1.26	1.12
H_2C**N**H	1.35	0.66	1.36	0.68
H_2**C**NH	1.38	0.73	1.42	0.67
H_2**CN**H	1.52	0.59	1.59	0.60

the energy for creation of bonds between adsorbate and surface. It is also influenced by the changes in the geometry within the surface and adsorbate, respectively. Indeed, in the present study, only the surface atoms closest to the adsorbate were influenced geometrically upon adsorption (Sec. II), but the geometry within the adsorbate was in many cases found to change considerably. More specifically, the adsorption of CN (by either the C or N atom) was found to be fully associative. As a result of adsorption of **C**N to the Si(C) surface, the internal C-N bond population was even found to increase (pop[r_2(ads)]$-$pop[r_2(gas)]$=$0.13 (0.19) |e|, Table V). The strong C-N bond explains in part why the extremely strong **C**N adsorption energies [503(511) kJ/mol] obtained were not correlated with extremely strong bonds to the surface. Furthermore, the C-N distance (r_2) of HCN, H_2CNH (bonded to the surface by either the C or N atom), and H**N**C was stretched [r_2(ads)$-r_2$(gas)$=$0.07–0.16 Å] as a result of the geometry optimization calculations (Table V). The corresponding overlap populations decreased simultaneously (pop[r_2(ads)]$-$pop[r_2(gas)]$=-$0.34$-$0.51 |e|), confirming a considerable weakening of the internal bonds of the adsorbates. HN**C** dissociated only slightly. The internal bond stretching explains in part why the bonds of HCN, H**N**C, and H_2CNH to the SiC surfaces are stronger than the corresponding adsorption energies suggest.

2. Twofold adsorption

As mentioned in Sec. III B 2, it is important to compare the processes of onefold and twofold adsorption. Hence, calculations for twofold adsorption of HCN, HNC, CN, and H_2CNH were also carried out and the numerical order of energies for the Si surface is

$$\mathbf{CN}(463) > H_2\mathbf{CN}H(395) > H\mathbf{CN}(300) > H\mathbf{NC}(225). \tag{8}$$

The corresponding order for the C surface is

$$\mathbf{CN}(522) > H_2\mathbf{CN}H(236) \sim H\mathbf{CN}(220) > H\mathbf{NC}(169). \tag{9}$$

The twofold adsorption reactions of **CN**, H**CN**, H**NC**, and H_2**CN**H were all found to be exothermic and the corresponding adsorption energies were of the same numerical order for the two different surfaces. Furthermore, the adsorption energies obtained for H**CN**, H**NC**, and H_2**CN**H were larger (by 70–163 kJ/mol) for the Si surface compared to the C surface. As a result of the calculations, the preferred adsorption of **CN** was found to be onefold to the C surface. When starting from **CN** in a position of twofold adsorption, the N atom in the adsorbate spontaneously desorbed from the C surface. Hence, the finally obtained adsorption energy for an initially twofoldly positioned **CN** molecule on the C surface corresponds to adsorption of **C**N to one of two neighboring surface radical sites. The result was also energetically and geometrically very similar to the situation for one fold adsorption of **C**N (Table IV). To the Si surface, **CN** was found to chemisorb strongly, even if the calculated twofold adsorption energy (463 kJ/mol) is numerically similar to the onefold adsorption energy (503 kJ/mol) obtained for **C**N (Sec. III C 1). Moreover, after **CN** adsorption, the C atom in the adsorbate was found to bind stronger than the N atom to the Si surface. On the contrary, the sum of the two one-fold adsorption energies for HCN, HNC, and H_2CNH, respectively, were found to be much less favorable than the corresponding twofold adsorption energies. The important sp^3-hybridization of the bonding surface atom was maintained after twofold adsorption of all the present adsorbates ($\nu_{\text{C-Si-C}}/\nu_{\text{Si-C-Si}}=107.8$–$111.2°$, Table IV). This situation is different from onefold adsorption, for which the influence of sp^2 hybridization on the bonding surface atom was stronger after adsorption of some of the adsorbates (i.e., C**N**, **C**N, H**C**N^{Si}, HN**C**$^{\mathrm{Si}}$, or H**N**C).

A correlation between shorter bond length, larger overlap population and relatively stronger adsorption energies has been observed for the present adsorption processes. The bonds between each of the atoms in the adsorbate and their closest surface atom were generally found to be weaker after twofold than after onefold adsorption. However, the individual bonds of H_2**CN**H to the Si surface seemed to be similar or stronger for twofold compared to onefold adsorption. The internal bond in H_2**CN**H was much more stretched (by 0.14–0.23 Å) after twofold compared to onefold adsorption (Table IV). For the remaining adsorbates (except **CN**$^{\mathrm{C}}$) the internal bond was also more stretched (by 0.05–0.10 Å) after twofold adsorption.

3. Discussion

Chemisorption of CN to the SiC(0001) surfaces was found to be strongly exothermic, with the exception of twofold adsorption to the C surface. However, since the energy for twofold adsorption of CN to the Si surface was of the same order of magnitude as for each of the individual onefold CN adsorption energies, twofold adsorption of CN does not seem to be advantageous to either surface. In all cases studied (except **CN**$^{\mathrm{C}}$), the adsorption of CN was energetically more favorable than adsorption of HCN, HNC, or H_2CNH. Unlike the situation for CN, the sum of the onefold adsorption energies for HCN, HNC and H_2CNH, respectively, was found to less favorable than the corresponding twofold adsorption energy. For HCN, HNC, H_2CNH, the direct twofold adsorption mechanism is plausible. Among the onefold adsorption energies, only those for C**N**, **C**N, HN**C**, HC**N**$^{\mathrm{Si}}$, and H_2CNH^{Si} were calculated to be larger than 100 kJ/mol. For these situations, onefold adsorption followed by a sequential adsorption of the second atom of the adsorbate, is an additional possible pathway for twofold adsorption. Furthermore, while there in some cases (i.e., C**N**, **C**N, H**C**N^{Si}, HN**C**$^{\mathrm{Si}}$, or H**N**C) was an influence of sp^2 hybridization on the binding surface atom after one adsorption, the surface atoms were generally sp^3 hybridized as a result of twofold adsorption. Moreover, all the twofold adsorption energies were numerically larger for the Si surface.

For equilibrium conditions, HCN and HNC have been predicted to be more abundant (with concentrations 10–10^2 times lower than N_2) than CN or H_2CNH (10^6 times lower than N_2) in the gas phase during SiC growth [Eqs. (2),(3)]. From the results in the present article, one can conclude that HCN and HNC do not adsorb strongly to the SiC(0001) surfaces. However, these species do bind to the surfaces at 0 K. This fact can make them important dopant contributors if the corresponding growth mechanisms (i.e., adsorption/desorption barriers, migration barriers, etc.) are advantageous. It is difficult to predict if HCN or HNC will adsorb favorably on the SiC surfaces at experimental temperatures. However, adsorption of CN (as well as of H_2CNH to the Si surface) is energetically much more advantageous and cannot be ruled out as a contributing factor for incorporation of nitrogen for the reasons discussed in Sec. III C 3.

D. Adsorption of SiN, SiNH, Si_2N

1. Onefold adsorption

The energies for onefold adsorption of SiN, SiNH, and Si_2N to the Si plane of SiC(0001) have also been calculated (Table I) and the numerical order of the energies obtained is

$$\begin{aligned}\mathrm{Si}\mathbf{N}(650)&>\mathrm{Si}_2\mathbf{N}(348)\sim\mathrm{Si}\mathbf{N}(340)>\mathbf{Si}_2\mathrm{N}(283)\\&>\mathrm{Si}\mathbf{N}\mathrm{H}(235)>\mathbf{Si}\mathrm{NH}(144).\end{aligned}\tag{10}$$

The corresponding energies for the C surface is

$$\begin{aligned}\mathrm{Si}\mathbf{N}(546)&>\mathbf{Si}_2\mathrm{N}(402)\sim\mathbf{Si}\mathrm{N}(385)>\mathrm{Si}_2\mathbf{N}(250)\\&>\mathbf{Si}\mathrm{NH}(211)>\mathrm{Si}\mathbf{N}\mathrm{H}(122).\end{aligned}\tag{11}$$

The calculated adsorption energies were all exothermic. The N atom in each of the adsorbates (Si**N**, Si**N**H, Si_2**N**) was found to preferentially bind to the Si surface (with adsorption energies stronger by 98–113 kJ/mol). On the contrary, the Si atom of the adsorbates (**Si**N, **Si**NH, **Si**$_2$N) was found to form relatively stronger bonds (by 45–119 kJ/mol) to the C surface. In summary, of all the adsorption reactions discussed in the present study, only those for **Si**N, **Si**NH, **Si**$_2$N and the radical N adsorbate (Sec. III B 1) were found to be more exothermic for the C surface compared to for the Si surface. As can be seen in Table VI, almost all of the present adsorption reactions resulted in a predominant sp^3 hybridization of the adsorbate-bonding surface atom. The binding surface Si atom was partly sp^2 hybridized ($\nu_{\text{C-Si-C}}=111.6°$) after adsorption of **Si**N.

Also for these species, the stronger adsorption energies correspond to relatively shorter bond lengths with larger overlap populations (Table VI). Futhermore, on the analogy of C**N** (Sec. III C 1), the internal bond of Si**N** was strengthened by adsorption to the Si (C) surface. More specifically, the internal bond length (r_2) altered only little [by 0 (0.04) Å] and the corresponding overlap population increased [by 0.46 (0.52) $|e|$] as a result of adsorption (Table VII).

TABLE VI. The distance between the adsorbate and the surface r_1 (Å), the overlap population in the bonding region pop$[r_1]$ ($|e|$) and the angle between the adsorbate-bonding surface Si(C) atom and its closest C(Si) neighbors $\nu_{\text{C-Si-C}}$ ($\nu_{\text{Si-C-Si}}$) (deg). Where two atoms in the adsorbate bind to the surface, the values corresponding to the N atom in the adsorbate are listed first.

		Si surface			C surface	
	r_1	pop$[r_1]$	$\nu_{\text{C-Si-C}}$	r_1	pop$[r_1]$	$\nu_{\text{C-Si-C}}$
Term.	1.51	0.94	110.7	1.12	0.80	111.3
Rad.			112.6			115.6
Dirad.			113.5			114.9
			/113.3			/115.0
Si**N**	1.69	0.71	109.7	1.41	0.72	109.3
SiN	2.39	0.71	111.6	1.82	0.61	110.5
SiN	1.68	0.78	108.4	1.40	0.70	110.3
	/2.74	/0.39	/112.0	/2.01	/0.40	/110.6
Si**N**H	1.74	0.62	110.7	1.54	0.54	109.9
SiNH	2.44	0.63	110.8	1.86	0.54	110.6
SiNH	1.75	0.64	108.3	1.54	0.53	109.2
	/2.49	/0.67	/110.1	/1.93	/0.54	/110.3
Si$_2$**N**	1.73	0.65	110.9	1.47	0.61	108.6
Si$_2$N	2.41	0.70	108.3	1.87	0.54	108.8
Si$_2$N	1.72	0.68	108.1	1.49	0.58	110.2
	/2.41	/0.76	/109.8	/1.95	/0.50	/108.6

2. Twofold adsorption

The order of the adsorption energies for twofold adsorption of SiN, SiNH, and Si$_2$N to the Si plane was calculated to be

$$\mathbf{SiN}(662) > \mathbf{Si_2N}(494) > \mathbf{SiN}\mathrm{H}(453). \tag{12}$$

The corresponding order for the C plane is

$$\mathbf{SiN}(561) > \mathbf{Si_2N}(393) \sim \mathbf{SiN}\mathrm{H}(391). \tag{13}$$

As can be seen above, all the calculated adsorption energies were strongly exothermic and somewhat larger (by 62–101 kJ/mol) for the Si surface than for the C surface. The sum of the two onefold adsorption energies for SiN and Si$_2$N, respectively, was found to be more favorable than the corresponding twofold adsorption energy. The opposite relation between the onefold and twofold adsorption energies was found for SiNH. Furthermore, the angles in the structural region below the adsorbates ($\nu_{\text{C-Si-C}}/\nu_{\text{C-Si-C}} = 108.3°–110.6°$) imply fairly good sp^3 hybridization of the bonding surface atoms. The exception is that the Si surface atoms become partly sp^2 hybridized ($\nu_{\text{C-Si-C}} = 112.0°$) upon adsorption of the Si atom in **SiN** (Table VI). This is similar to onefold adsorption of **Si**N, where the surface atom was found to be partly sp^2 hybridized (Sec. III D 1).

For each of the adsorption reactions presented in this section, the distance between the binding surface atom and the N atom in the adsorbate, as well as the corresponding bond population, was similar for onefold and twofold adsorption processes. On the contrary, the bond to the surfaces by the Si atom in **SiN**, **SiN**H, and **Si$_2$N**, respectively, was weaker in the case of twofold adsorption. This (Si-Si) bond was particularly weak after adsorption of **SiN**. Twofold adsorption of SiN is, hence, dominated by the bond created between the N atom and the surface. This is similar to what was found for twofold adsorption of CN (Sec. III D 2).

TABLE VII. The distance between the non-H atoms in the adsorbate r_2 (Å) and the corresponding overlap population pop$[r_2]$ ($|e|$).

	Si surface		C surface	
	r_2	pop$[r_2]$	r_2	pop$[r_2]$
SiN	1.55	0.90	1.55	0.90
Si**N**	1.55	0.90	1.59	0.93
SiN	1.55	1.36	1.59	1.42
SiN	1.59	0.85	1.65	0.78
SiNH	1.52	0.82	1.52	0.82
Si**N**H	1.69	0.40	1.70	0.49
SiNH	1.56	0.86	1.58	0.88
SiNH	1.73	0.52	1.74	0.64
Si$_2$N	1.66	0.35	1.66	0.35
Si$_2$**N**	1.75	0.32	1.75	0.37
Si$_2$N	1.66	0.52	1.69	0.49
	/1.56	/0.76	/1.56	/0.77
Si$_2$N	1.88	0.18	1.83	0.37
	/1.67	/0.41	/0.69	/0.41
	/2.30	/0.46	/2.44	/0.21

3. Discussion

SiN, Si$_2$N, and SiNH were all found to chemisorb to the SiC(0001) surfaces. Stronger adsorption was obtained for SiN and the weaker adsorption was obtained for SiNH. The present adsorbates were found to bind relatively stronger by the N atom to the Si surface, and by the Si atom to the C surface. The sum of the energies for onefold adsorption of SiNH was larger than the corresponding energy for twofold adsorption. Hence, for this species, onefold adsorption can be followed by twofold adsorption by a sequential "bending-over" adsorption process. On the contrary, the onefold and twofold adsorption energies for SiN and Si$_2$N, respectively, were similar, and for these adsorbates twofold adsorption does not seem to be advantageous. Moreover, the binding surface atom was fairly well sp^3 hybridized after adsorption of each of the species, except for **Si**N(**SiN**) to the Si surface, for which it was partly sp^2 hybridized.

From thermodynamic calculations at equilibrium conditions, the concentrations of SiN and Si$_2$N have been predicted to be higher (10^3 times lower than that of N$_2$) compared to SiNH (10^6 times lower than N$_2$), see Eqs. (2),(3). However, SiN and Si$_2$N were not predicted to form close to the surface, according to Eq. (2). Hence, SiNH is likely to be more abundant (but still very rare) than SiN and Si_2N close to the growing SiC surface. However, because of their favorable adsorption processes, SiN or Si_2N can be made abundant, e.g., by assistance of laser or hot filament of the gaseous atmosphere in the reactor, these species can become important for N incorporation into SiC.

IV. CONCLUSIONS

The nitrogen-containing species N, N_2, NH_3, NH_2, CN, HCN, HNC, H_2CNH, SiN, SiNH, Si_2N have, from thermodynamic calculations[9] been predicted to be present in the gaseous atmosphere during growth of nitrogen-doped SiC. In order to investigate the incorporation of nitrogen into SiC surfaces, the adsorption of these species onto SiC(0001) surfaces has been studied theoretically, using DFT calculations under periodic boundary conditions.

Chemisorption of N, NH_2, CN, SiN, or Si_2N was found to be strongly exothermic to both SiC surfaces. For these species, the twofold adsorption energies were smaller than the sum of the corresponding onefold adsorption energies. Moreover, the structure of the binding surface atom was not favorably maintained after onefold adsorption of CN to either surface, and after adsorption of N, NH_2 or the Si atom in SiN to the Si surface. The remaining adsorption processes (involving N_2, NH_3, HCN, HNC, H_2CNH, and SiNH) were found to be energetically less favorable, but still exothermic (with the exception of NH_3, HC**N**, or H**N**C adsorbed to the C surface). Direct twofold adsorption is possible for this latter group of adsorbates (except NH_3), since twofold adsorption was found to be more exothermic than the two corresponding onefold adsorption reactions. One-fold adsorption, with a sequential adsorption of the second non-H atom in the adsorbate, seems to be another possibility for N_2, $HC\mathbf{N}^{Si}$, H**N**C, $H_2C\mathbf{NH}^{Si}$, and SiNH. For this latter group of adsorbates, the sp^3 hybridization of the binding surface atom was, with exception of N_2^{Si}, NH_3, $H\mathbf{C}N^{Si}$, H**N**C, $HN\mathbf{C}^{Si}$ maintained. For all the species in the present study, the twofold adsorption processes were found to be energetically more favorable for the Si than for the C surface. Adsorption by the N(Si) atom in the adsorbate, except for the N radical, was found to be stronger to the Si(C) surface while the adsorbates seem to bind equally strongly to both surfaces by the C atom. According to the site-competition technique, the N-containing species is "out-competed" by the C growth species on the Si (but not on the C) surface at high C/Si ratios. A plausible explanation for these experimental results can be that the N atom is implanted into the Si and C planes of the growing SiC material by adsorption of different atoms in the same adsorbate. From the present results, SiNH was found to bind stronger by the Si atom than by the *N* atom to the C surface. Incorporation of this species by the Si atom puts the N atom in the C site of the SiC lattice, a situation which experimentally has been found to be preferred.[6,7] Furthermore, SiNH was found to bind stronger by the N atom to the Si surface. This would also put N in the C site of the lattice. By an increase in C precursors, the N incorporation process is out competed by adsorption of C-containing species to the Si surface. It is plausible that the adsorption (by the Si atom) of SiNH is more similar to that of the Si growth species to the C surface. Further investigations are, however, needed in order to confirm this proposed mechanism.

Bonds are expected to become weaker with an increase in temperature. It is difficult to predict whether N_2 or NH_3, HCN, and HNC (with concentrations $10–10^3$ times lower than N_2) or H_2CNH and SiNH (with concentrations 10^6 times lower than N_2) adsorb at experimental temperatures [Eqs. (2),(3)]. If N_2 or NH_3, HCN, and HNC do adsorb, they do not bind strongly (especially not to the C surface), but they may bind sufficiently strongly. The gaseous species N, NH_2, CN, SiN, and Si_2N, which energetically have much more favorable adsorption reactions, are predicted to be quite rare (i.e., with concentrations $10^5–10^8$ times lower than the concentration of N_2). According to a novel study by Danielsson and co-workers,[18] using and elaborated model which describes the conditions in a CVD reactor, N_2 has been predicted to be the only plausible species for N incorporation into SiC during *in situ* growth. According the present results, the internal N-N bond weakens by adsorption, abstraction reactions with gaseous H radicals may facilitate that mechanism. However, N_2 has presently also been found to adsorb very weakly to the C surface, which experimentally has been found to be more favorable for N incorporation than the Si surface. The mechanisms for N incorporation are very complex and further studies are needed in order to understand them. It is then also important to keep in mind that although thermodynamic calculations give good indications, the gaseous composition in a CVD reactor is not in equilibrium. Furthermore, it is possible to control the gas mixture by activation of the precursor gas during deposition (e.g., by laser or hot filament) and thereby change the composition of gaseous species significantly. This possibility justifies the inclusion in this study of also the N-containing species that have been predicted to occur in relatively low concentrations in a CVD reactor at equilibrium conditions.

ACKNOWLEDGMENTS

This paper was supported by the Swedish Research Council for Engineering Sciences (TFR), and the Ångstrom consortium. The results were generated using the program Cerius^{2TM}. This program was developed by Accelrys, Inc., San Diego.

---

[1] R. Davies, G. Kelner, M. Shur, J. W. Palmour, and J. A. Edmond, Proc. IEEE **79**, 677 (1991).

[2] G. Aylward and T. Finlay, *SI Chemical Data*, 3rd ed. (Wiley, Singapore, 1994).

[3] F. Bechstedt, P. Käckell, A. Zywietz, K. Karch, B. Adolph, K. Tenelsen, and J. Furthmüller, Phys. Status Solidi B **202**, 35 (1997).

[4] N. Sieber, B. F. Mantel, T. Seyller, J. Ristein, L. Ley, T. Heller, D.

Batchelor, and D. Schmeisser, Appl. Phys. Lett. **78**, 1216 (2001).
[5] T. Kimoto, A. Itoh, and H. Matsunami, Appl. Phys. Lett. **67**, 2385 (1995).
[6] H. H. Woodbury and G. W. Ludwig, Phys. Rev. **124**, 1083 (1961).
[7] P. Deák, A. Gali, J. Miró, R. Guiterrez, A. Sieck, and T. Frauenheim, Mater. Sci. Forum **264-268**, 279 (1998).
[8] D. J. Larkin, Phys. Status Solidi B **202**, 305 (1997).
[9] U. Forsberg, Ö. Danielsson, A. Henry, M. K. Linnarsson, and E. Janzén, J. Cryst. Growth **236**, 101 (2002).
[10] P. Hohenberg and W. Kohn, Phys. Rev. **136**, B864 (1964).
[11] W. Kohn and L. J. Sham, Phys. Rev. **140**, A1133 (1965).
[12] J. Perdew and Y. Wang, Phys. Rev. B **45**, 13 244 (1992).
[13] L. Kleinman and D. Bylander, Phys. Rev. Lett. **48**, 1425 (1982).
[14] H. Monkhorst and J. D. Pack, Phys. Rev. B **13**, 5188 (1976).
[15] M. D. Segall, R. Shah, C. J. Pickard, and M. C. Payne, Phys. Rev. B **54**, 16 317 (1996).
[16] T. Aigo, M. Kanaya, M. Katsuno, H. Yashiro, and N. Ohtani, Jpn. J. Appl. Phys. **40**, 2155 (2001).
[17] M. Frenklach, Phys. Rev. B **45**, 9455 (1992).
[18] Ö. Danielsson, U. Forsberg, and E. Janzén, J. Cryst. Growth (to be published).